

Many-body Green's function GW and Bethe-Salpeter study of the optical excitations in a paradigmatic model dipeptide

C. Faber,^{1,2} P. Boulanger,¹ I. Duchemin,² C. Attaccalite,¹ X. Blase¹¹

¹*Institut Néel, CNRS and Université Joseph Fourier, B.P. 166, 38042 Grenoble Cedex 09, France.*

²*INAC, SP2M/L_sim, CEA cedex 09, 38054 Grenoble, France.*

(Dated: 4 September 2013)

We study within the many-body Green's function GW and Bethe-Salpeter formalisms the excitation energies of a paradigmatic model dipeptide, focusing on the four lowest-lying local and charge-transfer excitations. Our GW calculations are performed at the self-consistent level, updating first the quasiparticle energies, and further the single-particle wavefunctions within the static Coulomb-hole plus screened-exchange approximation to the GW self-energy operator. Important level crossings, as compared to the starting Kohn-Sham LDA spectrum, are identified. Our final Bethe-Salpeter singlet excitation energies are found to agree, within 0.07 eV, with CASPT2 reference data, except for one charge-transfer state where the discrepancy can be as large as 0.5 eV. Our results agree best with LC-BLYP and CAM-B3LYP calculations with enhanced long-range exchange, with a 0.1 eV mean absolute error. This has been achieved employing a parameter-free formalism applicable to metallic or insulating extended or finite systems.

I. INTRODUCTION

Charge-transfer (CT) excitations, i.e. the creation of an excited electron and hole with weakly overlapping spatial distributions, are a crucial feature in donor-acceptor systems, important e.g. for photovoltaic applications. Indeed, in organic photovoltaic cells, the separation of the strongly bound photogenerated electron-hole pairs is believed to take place at the donor-acceptor interface through an intermediate CT excited state.¹⁻³ However, the exact mechanisms leading to charge separation remain rather controversial,⁴⁻⁶ urging for computational quantum mechanical studies which allow an accurate exploration of local and CT excitations at various energies.

Treating CT excitations theoretically using *ab initio* methods remains difficult. Wavefunction-based quantum chemistry methods such as multiconfigurational techniques, e.g. complete active space second order perturbation theory (CASPT2) or multi-reference configuration interaction (MRCI),⁷ yield accurate results, but they are computationally too demanding to treat systems with more than a few tens of atoms. At the density functional theory (DFT) level, constrained DFT formalisms^{8,9} have proven to be extremely efficient in providing a good description of the lowest-lying CT excitation in rather large systems, but generalizing such techniques to higher excited states remains a difficult issue. Further, excited states wavefunctions, needed to calculate e.g. transfer rates, are not available. Using time-dependent density functional theory (TDDFT),¹⁰⁻¹² one obtains the entire excitation spectrum of systems significantly larger than that amenable to e.g. CASPT2 or MRCI approaches. However, it fails in most instances in reproducing CT excitations when standard (semi)local functionals are used.¹³⁻¹⁵ Such difficulties paved the way for the success of range-separated hybrid functionals¹⁶⁻¹⁹ that are precise for both local and CT excitations,²⁰⁻²⁴ even though the transferability from one system to another of the parameters controlling the short- and long-range exchange contributions remains a difficult issue.²⁵⁻²⁷

Recently, an alternative approach derived from many-body perturbation theory (MBPT) within a Green's function formalism, the so-called GW ²⁸⁻³⁴ and Bethe-Salpeter (BSE)³⁵⁻⁴¹ formalisms, initially developed and extensively tested for bulk semiconductors, has been applied successfully to the problem of CT excitations in gas phase organic systems. An accuracy of 0.1-0.15 eV as compared to experiment could be obtained for small gas phase donor-acceptor systems combining acenes and acene derivatives with the tetracyanoethylene

(TCNE) acceptor.^{42,43} Further, a similar agreement with coupled cluster (CC2) calculations⁴⁴ was obtained for intramolecular CT excitations in a coumarin family of interest for dye-sensitized solar cells.⁴⁵ The accuracy of the *GW*/BSE approach was demonstrated to be equivalent to that of TDDFT calculations with range-separated hybrid functionals and optimized parameters, but with a parameter-free formalism providing equivalent accuracy for extended and finite size systems. However, the number of *GW*/BSE studies of CT excitations in gas phase organic systems remains very scarce and much work is still needed to benchmark the approach on a large variety of molecules.

In the present study, we explore within the *GW*/BSE formalism a small - even though delicate - system, namely a model dipeptide based on the N-methylacetamide (C_3H_7NO) molecule (see Fig. 1a). This system denotes one of the first cases where large errors have been observed at the TDDFT level, triggering its study by a large variety of approaches, including CASPT2,⁴⁶ TDDFT with various (semi)local, hybrid or range-separated functionals^{22,47} and also a Bethe-Salpeter study based on an "empirical" *GW* approach.⁴⁸ Difficulties were encountered to reproduce the CASPT2 results⁴⁶ with unusual discrepancies between the mentioned state-of-the-art techniques. Moreover, a very large sensitivity of CT excitation energies on the chosen functional parameters within e.g. the same CAM-B3LYP TDDFT framework was observed.^{22,47}

In this work, we emphasize in particular the effect of self-consistency within the *GW* formalism, updating both quasiparticle energies and further single-particle wavefunctions within the so-called self-consistent Coulomb-hole plus screened-exchange (COHSEX) static approximation to *GW*.⁴⁹ Important level reorderings are observed, as compared to Kohn-Sham DFT calculations with semilocal functionals, which leads to important changes in the absorption spectrum. The effect of updating the wavefunctions within self-consistent COHSEX is shown to be more marginal. Our (singlet) excitation energies show an excellent agreement with existing CASPT2 calculations for most local and CT excitations, with a maximum error of 0.07 eV, except for a CT state shown to be blue shifted by up to 0.5 eV as compared to CASPT2. Overall, our results agree best with CAM-B3LYP calculations with an "enhanced" long-range exchange ($\alpha + \beta = 0.8$) contribution and the original LC-BLYP formulation, showing a maximum mean absolute error of 0.1 eV for both local and CT excitations.

II. METHODOLOGY AND TECHNICAL DETAILS

Developed in the mid-60s - and later extended at the *ab initio* level in the mid-80s - for the study of the electronic properties of extended semiconductors and insulators, the *GW* formalism²⁸⁻³⁴ is now starting to be applied to organic molecules in the gas phase in order to assess its merits and limitations.⁵⁰⁻⁶⁰ The *GW* approach aims at providing accurate quasiparticle energy levels, including the ionization energy and electronic affinity. As a brief overview, we introduce the non-local and energy-dependent self-energy operator $\Sigma(\mathbf{r}, \mathbf{r}'; E)$ that represents the effect of exchange and correlation in a generalized eigenvalue equation:

$$\left(\frac{-\nabla^2}{2} + V^{ion}(\mathbf{r}) + V^H(\mathbf{r}) \right) \phi_n(\mathbf{r}) + \int d\mathbf{r}' \Sigma(\mathbf{r}, \mathbf{r}'; E_n) \phi_n(\mathbf{r}') = E_n \phi_n(\mathbf{r}), \quad (1)$$

where V^{ion} and V^H stand for the ionic and Hartree potential, respectively. The self-energy operator Σ includes all interactions beyond the Hartree contribution. In the so-called *GW* approximation, it is simplified to:

$$\begin{aligned} \Sigma(\mathbf{r}, \mathbf{r}'; E) &= \frac{i}{2\pi} \int d\omega e^{i\omega 0^+} G(\mathbf{r}, \mathbf{r}'; E + \omega) W(\mathbf{r}, \mathbf{r}'; \omega), \\ G(\mathbf{r}, \mathbf{r}'; E) &= \sum_n \frac{\phi_n(\mathbf{r}) \phi_n^*(\mathbf{r}')}{E - \varepsilon_n + 0^+ \times \text{sgn}(\varepsilon_n - E_F)}, \\ W(\mathbf{r}, \mathbf{r}'; \omega) &= \int d\mathbf{r}'' \epsilon^{-1}(\mathbf{r}, \mathbf{r}''; \omega) V^C(\mathbf{r}'', \mathbf{r}'), \\ &= V^C(\mathbf{r}, \mathbf{r}') + \iint d\mathbf{r}'' d\mathbf{r}''' V^C(\mathbf{r}, \mathbf{r}'') \chi_0(\mathbf{r}'', \mathbf{r}''') W(\mathbf{r}''', \mathbf{r}'), \end{aligned}$$

with G is the time-ordered single-particle Green's function and W is the dynamically screened Coulomb potential. ϕ_n and ε_n are input single-particle eigenstates/eigenenergies, respectively, typically taken from DFT Kohn-Sham calculations (see below). E_F is the Fermi level and V^C the bare Coulomb potential. ϵ^{-1} denotes the inverse dynamical dielectric matrix, calculated here below within the random phase approximation, and χ_0 is the independent-electron susceptibility. The infinitesimally small positive value (0^+) is included when carrying out a Fourier transformation from time to frequency space to ensure convergence. For the sake of comparison, the non-local, but energy-independent (instantaneous), exchange Fock operator reads :

$$\Sigma^X(\mathbf{r}, \mathbf{r}') = \frac{i}{2\pi} \int d\omega e^{i\omega 0^+} G^{HF}(\mathbf{r}, \mathbf{r}'; \omega) V^C(\mathbf{r}, \mathbf{r}'), \quad (2)$$

where G^{HF} is built from Hartree-Fock single particle eigenstates.

Our GW calculations are performed with the FIESTA package,^{42,61,62} a recently developed Gaussian-basis implementation of the GW and Bethe-Salpeter formalisms. Dynamical screening and correlations are explicitly treated using contour deformation techniques without any plasmon-pole approximation (for more details on the contour deformation approach used, see 61 and 63). All non-local operators such as the independent-electron susceptibility χ_0 , the bare and screened Coulomb potentials V^C and W and the self-energy are expressed in terms of a large auxiliary atom-centered Gaussian basis combined with standard resolution-of-the-identity techniques.⁶⁴⁻⁶⁶ All unoccupied states, as appearing in the Green's function and independent-electron susceptibility, are included in the summation over empty states. The used auxiliary basis is composed of six primitive Gaussian functions ($e^{-\alpha r^2}$) per l -channel, up to $l=2$ orbitals for first row elements, with an even tempered distribution⁶⁷ of the localization coefficients (α) ranging from $\alpha_{min}=0.10$ Bohr⁻² to $\alpha_{max}=3.2$ Bohr⁻².

Our starting input eigenstates/energies (ϕ_n, ε_n) are taken from DFT Kohn-Sham calculations using the SIESTA DFT code⁶⁸ within the local density approximation (LDA)⁶⁹⁻⁷¹ combined with standard norm-conserving pseudopotentials.⁷² A large triple-zeta plus double polarization basis (TZDP) is used to converge the correlation contribution to the self-energy (see note 73 and 74 for details). The influence of the starting eigenstates onto the final quasiparticle energies has recently become a subject of study,^{61,75} starting with the observation that the standard "single-shot" perturbative G_0W_0 calculations, i.e. GW calculations based on Kohn-Sham LDA or PBE eigenstates/energies, tend to underestimate the gap of organic molecules.^{58,61,75} To remedy this problem, our GW calculations are performed in a partially self-consistent way, where the obtained quasiparticle energies are reinjected into the calculation of the time-ordered Green's function and the screened Coulomb potential W , whereas the wavefunctions are left unchanged. As emphasized in several recent works, this approach yields quasiparticle energies,^{58,61,62,76,77} electron-phonon coupling constants^{78,79} and optical absorption spectra^{42,43} in much better agreement with experiment than non-selfconsistent single-shot G_0W_0 calculations based on a starting LDA Kohn-Sham spectrum.

To study the influence of the input wavefunctions on the quasiparticle energies, we introduce a scheme which is widely used in the GW community for extended solids, namely a

fully-self-consistent approach where both eigenstates and eigenfunctions are updated using the so-called static Coulomb-hole plus screened-exchange (COHSEX) approximation to the self-energy operator (see Ref. 80 for details). The resulting modified eigenstates are then used to perform partially self-consistent GW calculations updating the quasiparticle energy levels, but freezing the self-consistent COHSEX wavefunctions.

Subsequently to the calculation of the quasi-particle spectrum using the GW formalism, the (screened) Coulomb interaction between excited electrons and holes can be taken into account within the Bethe-Salpeter (BSE) formalism.³⁵⁻³⁸ Here, the neutral excitation energies are the eigenvalues of the following electron-hole Hamiltonian equation:

$$\begin{pmatrix} R & C \\ -C^* & -R^* \end{pmatrix} \cdot \begin{pmatrix} [\phi_a(\mathbf{r}_e)\phi_i(\mathbf{r}_h)] \\ [\phi_i(\mathbf{r}_e)\phi_a(\mathbf{r}_h)] \end{pmatrix} = \begin{pmatrix} \lambda_{ai} \\ \mu_{ia} \end{pmatrix} \begin{pmatrix} [\phi_a(\mathbf{r}_e)\phi_i(\mathbf{r}_h)] \\ [\phi_i(\mathbf{r}_e)\phi_a(\mathbf{r}_h)] \end{pmatrix}, \quad (3)$$

where the indexes (i,j) and (a,b) indicate the occupied and virtual orbitals, and $(\mathbf{r}_e, \mathbf{r}_h)$ the electron and hole positions, respectively. In this block notation, the vector $[\phi_a(\mathbf{r}_e)\phi_i(\mathbf{r}_h)]$ represents all excitations (note e.g. that $\phi_a(\mathbf{r}_e)$ means that an electron is put into a virtual orbital), while the vector $[\phi_i(\mathbf{r}_e)\phi_a(\mathbf{r}_h)]$ represents all disexcitations.

The so-called resonant R part is Hermitian and reads:

$$R_{ai,bj} = \delta_{a,b}\delta_{i,j} \left(\varepsilon_a^{QP} - \varepsilon_i^{QP} \right) - \iint \phi_a(\mathbf{r}_e)\phi_i(\mathbf{r}_h)W(\mathbf{r}_e, \mathbf{r}_h)\phi_b(\mathbf{r}_e)\phi_j(\mathbf{r}_h) \, d\mathbf{r}_h d\mathbf{r}_e \\ + 2\eta \iint \phi_a(\mathbf{r}_e)\phi_i(\mathbf{r}_e)V^C(\mathbf{r}_e, \mathbf{r}_h)\phi_b(\mathbf{r}_h)\phi_j(\mathbf{r}_h) \, d\mathbf{r}_h d\mathbf{r}_e, \quad (4)$$

with $\eta = 1$ for the singlet states studied here ($\eta = 0$ for triplets). The quasiparticle energies $\varepsilon_{a,b,i,j}^{QP}$ are the GW quasiparticle energies, while the $\phi_{a,b,i,j}$ are the Kohn-Sham eigenfunctions or the self-consistent COHSEX wavefunctions depending on the preceding GW scheme (see above). Notice that the electron-hole interaction term involving the screened Coulomb potential W does not vanish for non-overlapping electron and hole states. In this limit, taking for sake of illustration the case (i=j=h) and (a=b=l), where h and l stand for the HOMO and LUMO state, one obtains:

$$R_{hl,hl}^{BSE} \rightarrow (\varepsilon_l^{GW} - \varepsilon_h^{GW}) - (1/\epsilon_M) \langle |\phi_l(\mathbf{r})|^2 |\phi_h(\mathbf{r}')|^2 V^C(|\mathbf{r} - \mathbf{r}'|) \rangle, \\ R_{hl,hl}^{TDDFT} \rightarrow (\varepsilon_l^{DFT} - \varepsilon_h^{DFT}) - (\alpha + \beta) \langle |\phi_l(\mathbf{r})|^2 |\phi_h(\mathbf{r}')|^2 V^C(|\mathbf{r} - \mathbf{r}'|) \rangle,$$

where we included the TDDFT CAM-B3LYP expression²² for sake of comparison. These equations have been derived in the long-range limit, reducing $W(r, r')$ to $V^C(r, r')/\epsilon_M$, where ϵ_M is the macroscopic dielectric constant, and setting to one the error function in the exact exchange contribution to the CAM-B3LYP functional. Clearly, through vacuum, where $\epsilon_M = 1$, the correct asymptotic limit⁸¹: $(IP - EA - 1/R)$, with IP being the ionization potential, EA the electronic affinity and R an average HOMO to LUMO distance, is recovered. In the CAM-B3LYP case, the correct asymptotic limit would require an $\alpha + \beta = 1$. We will come back to this point in the following.

Within the so-called Tamm-Dancoff approximation (TDA), the coupling between resonant (R) and anti-resonant (R^*) transitions is neglected, i.e. C and C^* are assumed to be zero. In the following, instead of applying the TDA, we diagonalize the full BSE matrix. As recently shown in several BSE studies,^{48,82-84} it is important to go beyond the TDA in nanosized systems, where it can lead to a blue-shift of the order of 0.3 eV. Finally, due to the quick increase in size of the $(\phi_a\phi_i)$ product basis, we include all occupied states but restrict the contributing transitions to the lowest-lying 160 unoccupied (virtual) states.⁸⁵ The accuracy of the present GW/BSE formalism and its implementation has been tested recently in the case of small donor-acceptor complexes, with a mean absolute error (MAE) of 0.1-0.15 eV as compared to experiment for low-lying excitations showing a clear CT character.⁴² It has been demonstrated that the results obtained with the present Gaussian basis implementation agree extremely well with planewave based GW/BSE calculations performed with the well established QuantumEspresso and Yambo code.^{86,87} Similarly, intramolecular CT excitations in a family of coumarins displayed a MAE within 0.06 eV as compared to coupled cluster (CC2) calculations.⁴⁵ We now address the delicate case of the dipeptide where, as shown below, significant differences have been observed between various methodologies.

III. RESULTS AND DISCUSSIONS

A. Notation

The model dipeptide studied here below was originally introduced in Ref. 46 and studied subsequently by a large variety of approaches^{22,47,48,88,89} as a test case for intramolecular CT excitations. The molecular structure⁹⁰ is represented in Fig. 1a and was relaxed at a DFT-

B3LYP⁹¹ level with a 6-311G(d,p) basis using the Gaussian09 package.^{73,92} The Kohn-Sham wavefunctions for states around the energy gap are depicted in Fig. 1b. It is primarily these states which contribute to the lowest-lying optical transitions. The listed states possess either σ - or π - character and are mainly localized on one side of the molecule or the other (denoted with a subscript $i = 1, 2$). The asterisk stands for unoccupied (virtual) states. In this publication, we focus on two different kinds of excitations. On the one hand, we are interested in valence transitions, labeled $W1$ and $W2$, between states localized on the same peptide unit, where the electron is promoted from an occupied σ_i -state to an unoccupied π_i^* -state. On the other hand, we study CT excitations between states localized on different peptide groups, namely the CTa exciton, a $\sigma_1 \rightarrow \pi_2^*$ transition, and the CTb exciton, a $\pi_1 \rightarrow \pi_2^*$ transition.

Anticipating on our GW /BSE results in section B and C, Fig. 2 illustrates the studied excitations by providing an isocontour representation of the hole-averaged electron distribution (transparent green) as obtained from the expectation value of the electron density operator $\delta(\mathbf{r} - \mathbf{r}_e)$ on the corresponding two-body $\psi(\mathbf{r}_e, \mathbf{r}_h)$ BSE eigenstate. Similarly, the electron-averaged hole distribution is represented (grey wireframe). The very clear CT character of the CTa transition and the partial CT character of the CTb excitation can be easily verified.

B. GW and Bethe-Salpeter calculations beyond the scissor operator

As discussed in the technical details section, we first perform self-consistency on the eigenvalues in our GW calculations, while leaving the Kohn-Sham wavefunctions unchanged. As expected, the DFT-LDA Kohn-Sham energy gap is significantly opened, from 4.6 eV to 11.9 eV within self-consistent GW . Beyond this known energy gap opening effect, important σ - and π -level crossings are observed for the highest occupied levels (see Fig. 3), with in particular a GW correction about 0.5 eV larger for the two σ - states than for the two π -levels. An important consequence is that the highest occupied molecular orbital (HOMO) changes its character from σ within DFT-LDA to π within GW . One can speculate that the stronger localization of the σ -orbitals leads to a larger self-interaction error as compared to π -orbitals, pushing them at too high energies at the DFT-LDA level. A similar effect has been noticed in a recent GW study on DNA/RNA nucleobases,^{62,93} where it has been

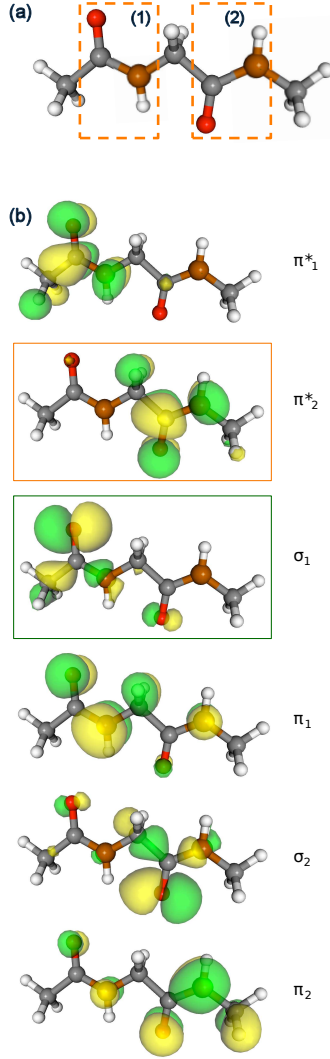
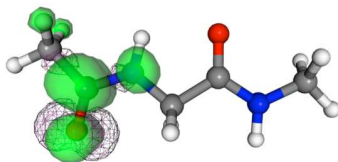
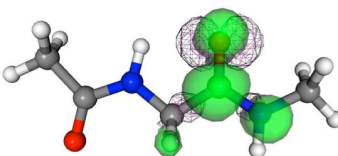


FIG. 1. (Color online) a) Symbolic representation of the studied model dipeptide, based on the N-methylacetamide (C_3H_7NO) molecule, in its planar geometry (see Ref. 46, structure 1a). The active peptide bonds ($C(O)NH$) are singled out in orange boxes. In CT excitations, the electron is promoted from one peptide group to the other. b) Isocontour representation of the Kohn-Sham wavefunctions around the gap classified by their σ - or π -character. The highest occupied molecular orbital (HOMO) and lowest unoccupied molecular orbital (LUMO) are singled out in a green and orange box, respectively. The asterisk denotes unoccupied orbitals, the subscripts (1, 2) the peptide unit on which the orbital is localized. The ordering corresponds to the DFT-LDA energy spectrum. Carbon atoms are represented in grey, oxygen in red, nitrogen in orange and hydrogen in white, respectively.

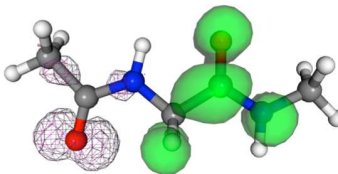
W1: $\sigma_1 \rightarrow \pi_1^*$



W2: $\sigma_2 \rightarrow \pi_2^*$



CTa: $\sigma_1 \rightarrow \pi_2^*$



CTb: $\pi_1 \rightarrow \pi_2^*$

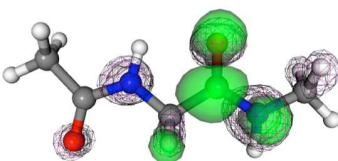


FIG. 2. (Color online) Isocontour representation in green (wireframe) of the averaged electron (hole) distribution for the valence transitions W_i ($\sigma_i \rightarrow \pi_i^*$), the CTa ($\sigma_1 \rightarrow \pi_2^*$) and the CTb ($\pi_1 \rightarrow \pi_2^*$) excitations. Carbon atoms are represented in grey, oxygen in red, nitrogen in blue and hydrogen in white, respectively.

shown that the present partially self-consistent GW scheme leads to quasiparticle energies in excellent agreement with high-level quantum chemistry *ab initio* coupled-cluster and multiconfigurational perturbation methods such as CCSD(T), CASPT2 and EOM-IP-CCSD.

A recent study of the dipeptide, by Rocca and coworkers,⁴⁸ used the BSE formalism directly on top of a DFT Kohn-Sham calculation, for which the LDA HOMO-LUMO gap has been opened by hand using an "empirical" value.⁹⁴ This rigid shift preserved the DFT-LDA ordering and energy spacing between occupied (unoccupied) orbitals, an approach

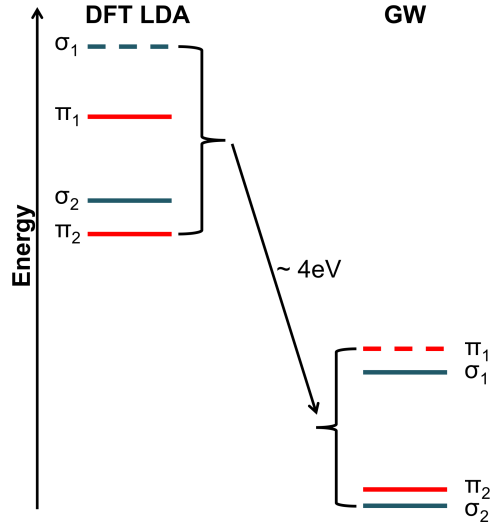


FIG. 3. (Color online) Qualitative representation of the highest occupied molecular orbitals level ordering within DFT-LDA and GW . In blue the σ - states and in red the π - states. The HOMO is highlighted with a dashed line. Note the energy reordering and the changed spacing between the levels.

labeled the "scissor" approximation to the GW self-energy. We now analyze the results of our Bethe-Salpeter calculations starting from a quasiparticle (GW) spectrum presenting a corrected level spacing and ordering.

C. Comparison to multi-reference quantum chemistry perturbation theory and TDDFT methods

In Table I and Fig. 4, we provide the excitation energies as obtained by our GW /BSE calculations for the local $W1$ and $W2$ and the charge-transfer CTa and CTb transitions. Our GW /BSE values are compared to standard TDDFT-LDA calculations performed both with the FIESTA code, using the same basis than for our BSE calculations, and the QuantumEspresso package^{48,86} using a planewave basis. Further, the results of previous TDDFT calculations using the hybrid B3LYP, the long-range corrected LC-BLYP and the Coulomb-attenuated CAM-B3LYP functionals with two different parametrisations^{22,47} are presented, together with an early quantum chemistry CASPT2 calculation.⁴⁶

Our TDDFT-LDA calculations come in very good agreement with the previous TDDFT-

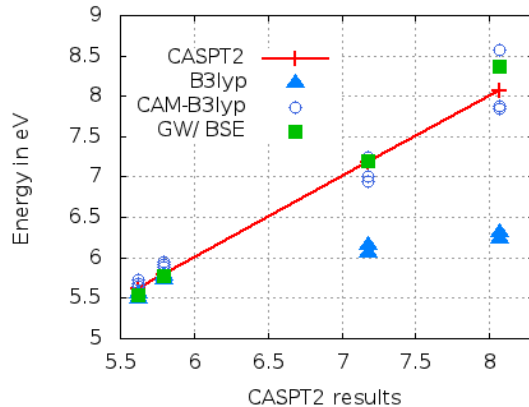


FIG. 4. (Color online) Excitation energies as provided within several theoretical frameworks plotted against the CASPT2 results (first diagonal in red). The TDDFT values with the B3LYP (blue up triangles) and the CAM-B3LYP (open circles) functionals, the present BSE calculations (green squares), starting from the $GW@LDA$ partially self-consistent eigenstates (see text), are represented. Several CAM-B3LYP values are found for each excitation, showing in particular the spread of values as a function of the $(\alpha + \beta)$ parameter. Energies are given in eV.

LDA planewave-based calculations performed with the QuantumEspresso package.⁴⁸ Both calculations predict CT states in nearly perfect agreement, with a negligible 0.02 eV discrepancy. The local $W1$ and $W2$ transitions agree within 0.1 eV. Such an agreement certainly comes as a good confirmation of the quality of the Kohn-Sham and auxiliary Gaussian bases used in the present study. Very similar results were also obtained at the TDDFT-PBE level in Ref. 47 with a maximum discrepancy of 0.05 eV as compared to our TDDFT-LDA calculations.

The main outcome of the TDDFT-LDA or TDDFT-PBE calculations is that CT excitation energies are much too small. The CT excitations are located below the lowest intramonomer $W1$ or $W2$ excitations. This is in great contrast to the CASPT2 results, where the CT excitations are found to lie about 1.4 eV to 2.4 eV above the $W1$ and $W2$ transitions. Our TDDFT-LDA value (4.63 eV) for the CTa transition, which consists nearly entirely of a transition between the Kohn-Sham highest occupied (HOMO) and lowest unoccupied (LUMO) molecular orbitals, can be compared to the HOMO-LUMO Kohn-Sham gap of 4.62 eV. This confirms that within TDDFT using local exchange-correlation functionals, the electron-hole interaction term vanishes for spatially separated electron and hole

states and one is left with the energy difference between Kohn-Sham states, neglecting any excitonic interaction. On the other hand, the local $W1$ and $W2$ transitions, with a strong overlap between final and initial states, are much better described, even though showing a 0.2-0.3 eV red shift for the $W1$ transition as compared to CASPT2.

Introducing some amount of exact exchange in addition to the charge-density-dependent TDDFT kernel yields a term similar to the BSE W matrix elements, but with the bare Coulomb potential V^C instead of the screened Coulomb potential W . As a result, even non-overlapping electrons and holes can interact. Previous TDDFT-B3LYP calculations (see Table I) indeed show some improvement as compared to TDDFT-LDA by locating the CT states above the $W1$ and $W2$ transitions. However, compared to CASPT2 calculations, the CT excitations energies are still about 1 eV to 1.8 eV too small, as a reminder that the B3LYP functional captures only 20% of the exact Fock exchange operator. This problem can be cured using range-separated functionals such as LC-BLYP or CAM-B3LYP, where the CT excitations come in much better agreement^{22,47} with the quantum-chemistry reference as indicated in Table I. Nevertheless, within the CAM-B3LYP method itself, one observes energy differences in the order of 0.7 eV for the CTa exciton, leading to the standard question of the proper choice of the needed parameters ($\alpha + \beta = 0.65$ or $\alpha + \beta = 0.8$ in the present case). This point will be discussed below.

Comparing our GW/BSE calculations (@LDA column in Table I) to CASPT2 values, we find an excellent agreement for the $W1$, $W2$ and the CTb exciton. The maximum discrepancy is 0.07 eV for the $W1$ transition, while remarkably both the local $W2$ and charge-transfer CTb excitation agree within 0.02 eV.⁹⁵ Clearly, tuning the (α, β) and range-separation parameters may bring the CAM-B3LYP calculations in better agreement with CASPT2 values, but we emphasize that the present GW/BSE scheme does not contain any adjustable parameters. Concerning the oscillator strengths of the respective transitions, the GW/BSE values are in reasonable agreement with the CASPT2 reference. The LC-BLYP and CAM-B3LYP values also agree for the transitions with vanishing oscillator strength, whereas they significantly underestimate the value of the oscillator strength for the CTb exciton, where the GW/BSE oscillator strength is closer to the CASPT2 value. As observed recently in a GW/BSE study of intramolecular CT excitations in the coumarin family,⁴⁵ obtaining an excellent agreement between the various formalisms proves more difficult for the oscillator strengths than for the corresponding excitation energies.

TABLE I. Singlet excitation energies for the model dipeptide as obtained within various TDDFT, many-body perturbation theory and CASPT2 approaches. Energies are in eV. For the CAM-B3LYP columns, the (0.65) and (0.8) numbers indicate the $(\alpha + \beta)$ parameter that controls in particular the percentage of long-range exchange. The @LDA and @COHSEX columns indicate that the (partially) self-consistent GW calculations, with update of the self-consistent eigenvalues only, have been performed with either DFT-LDA or self-consistent COHSEX eigenstates as a starting point. Numbers in parenthesis are the oscillator strengths. Oscillator strengths in the $(\alpha + \beta) = 0.65$ CAM-B3LYP column are taken from Ref. 22.

	TD-DFT				GW/BSE		CASPT2 ^d		
	LDA		B3LYP ^{b/c}	LC-BLYP	CAM-B3LYP				
	Ref ^a	Fiesta	Refs ^{b/c}	Ref. ^b	(0.65) ^{b/c}	(0.8) ^b	@LDA	@COHSEX	
<i>W1</i>	5.30	5.40	5.49/5.55	5.56 (.001)	5.65/5.68 (.001)	5.72 (.001)	5.55 (.001)	5.58 (.001)	5.62 (.001)
<i>W2</i>	5.66	5.73	5.73/5.77	5.80 (.000)	5.88/5.92 (.000)	5.95 (.000)	5.79 (.000)	5.80 (.000)	5.79 (.001)
<i>CTb</i>	5.15	5.13	6.06/6.15	7.02 (.043)	6.94/7.00 (.018)	7.24 (.040)	7.20 (.095)	7.13 (.063)	7.18 (.134)
<i>CTa</i>	4.61	4.63	6.24/6.31	8.38 (.000)	7.88/7.84 (.000)	8.58 (.000)	8.36 (.000)	8.58 (.000)	8.07 (.000)

^aRef. 48

^bRef. 22

^cRef. 47

^dRef. 46 (Table 2, structure 1a).

The largest discrepancy between the present $GW/BSE@LDA$ and available CASPT2 calculations is of 0.3 eV for the *CTa* excitation. For such a transition, our GW/BSE value is in nearly perfect agreement with the LC-BLYP prediction, lying in between the two CAM-B3LYP values. As evidenced in Table I and Fig. 4, observing the rather large ~ 0.7 eV variation between the two CAM-B3LYP values, such a transition is clearly very sensitive to the details of the exchange and correlation potential. Before commenting on such a deviation, we will test the impact of using frozen Kohn-Sham LDA eigenstates in the present GW and Bethe-Salpeter approach here below.

D. *GW*/*BSE* calculations starting from self-consistent COHSEX eigenstates

In an attempt to better understand this delicate system and to explore the accuracy of the present *GW*/*BSE* formalism, we finally test one of the common approximations in the *GW* community, namely the assumption that the Kohn-Sham and quasiparticle eigenfunctions strongly overlap, even though the energy gap may differ significantly. This has been demonstrated e.g. in the case of bulk silicon in the early days of *GW* calculations,³¹ justifying the practice of updating the quasiparticle energies while freezing the starting Kohn-Sham orbitals.

A well-known example, where such an approximation fails, is the case of systems combining delocalized (*s,p*) orbitals and tight *3d* levels such as transition metal oxides. Such a failure has been cured within a self-consistent *GW* approach, where both quasiparticle energies and wavefunctions are updated.^{96,97} In the case of atoms or small molecular systems, it has been demonstrated recently that fully self-consistent *GW* calculations^{98–100} lead to better quasiparticle properties (ionization potential, HOMO-LUMO gap, etc.) than standard perturbative G_0W_0 calculations based on frozen Kohn-Sham LDA or PBE eigenstates.

Due to high computational costs for performing fully self-consistent *GW* calculations, a scheme has been developed based on a simplified "static" approximation to the *GW* self-energy operator, the so-called static screened-exchange plus Coulomb-hole approximation already discussed in an early paper by Hedin,²⁸ where the *GW* approach for the interacting homogeneous electron gas was introduced. In such an approach, full self-consistency with an update of both eigenvalues and eigenfunctions is performed at the COHSEX level, followed by a *GW* calculation with self-consistency on the eigenvalues only.⁸⁰ Such a scheme, in the following labeled as *GW*@COHSEX, has been shown to yield excellent results in semiconductors combining extended and localized states,^{80,101} as recently demonstrated in the case of transparent conductive oxides and quaternary thin films for photovoltaics^{102,103} or bulk gold.¹⁰⁴ Very briefly, the two contributions to the COHSEX self-energy are:

$$\begin{aligned}\Sigma^{SEX}(\mathbf{r}, \mathbf{r}') &= - \sum_n^{occ} \phi_n(\mathbf{r}) \phi_n^*(\mathbf{r}') W(\mathbf{r}, \mathbf{r}'; \omega = 0), \\ \Sigma^{COH}(\mathbf{r}, \mathbf{r}') &= \frac{1}{2} W(\mathbf{r}, \mathbf{r}'; \omega = 0) \delta(\mathbf{r} - \mathbf{r}'),\end{aligned}$$

where the screened exchange Σ^{SEX} term is analog to the bare exchange Fock operator -

with a summation over states limited to the occupied manifold - but replacing the bare Coulomb potential by the screened one at zero frequency. The Coulomb hole Σ^{COH} is a local operator with no summations over the eigenstates. Such an approximation can be obtained by assuming that the poles of the inverse dielectric matrix are located at much higher energy than the typical electronic transition energies. Several demonstrations or interpretations have been proposed in e.g. Refs. 31, 49 and 80, including a time-domain analysis in the seminal paper by Lars Hedin.²⁸

Our findings concerning the self-consistent COHSEX run are consistent with previous observations on extended semiconductors,³¹ namely that the static COHSEX approximation overcorrects the energy gap. Our COHSEX HOMO-LUMO gap for the dipeptide is found to be 12.9 eV, instead of 4.62 eV within DFT-LDA and 11.8 eV for $GW@COHSEX$, respectively. Providing a first indication that updating the wavefunctions does not affect very significantly the quasiparticle energy spectrum, we see that the 11.8 eV $GW@COHSEX$ energy gap is in good agreement with the 11.9 eV $GW@LDA$ value previously found. For the sake of comparison, the Hartree-Fock HOMO-LUMO gap is found to be 13.85 eV (all-electron cc-pVTZ Gaussian09 value). Clearly, the COHSEX gap is much closer to the final GW value than the starting DFT-LDA HOMO-LUMO Kohn-Sham gap. As compared to GW calculations, the slightly too large COHSEX gap originates mainly from the HOMO which is located nearly one eV too low in energy (overbinding), while the LUMO is found to agree within 0.1-0.2 eV with the final GW value.¹⁰⁵

Besides the improved value of the energy gap, an important finding is that the self-consistent COHSEX approximation yields the correct ordering of states. In particular, the HOMO level is the π_1 state, located (0.25,0.74,0.99) eV above the σ_1 , π_2 and σ_2 states, respectively, to be compared to spacings of (0.26,0.75,0.97) eV within the final $GW@COHSEX$ value. Such an excellent agreement in level ordering and energy spacing, together with a better HOMO-LUMO gap, indicates that the COHSEX energy spectrum is certainly a better starting point for GW calculations as compared to the DFT-LDA Kohn-Sham Ansatz.

Inferring a better quality of the COHSEX eigenfunctions from the strongly ameliorated energy spectrum, as compared to Kohn-Sham DFT-LDA calculations, remains a difficult issue. However, concerning the delicate CTa transition, the analysis of the COHSEX σ_1 and π_2^* states indicates that they project within 99.8% and 98.9%, respectively, onto the corresponding LDA eigenstates. This shows that the Kohn-Sham and COHSEX eigenstates

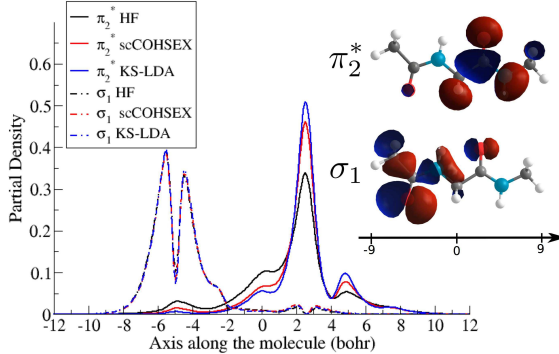


FIG. 5. (Color online) Comparison between the LDA (blue), COHSEX (red) and HF (black) wavefunctions for the σ_1 (dotted lines) and π_2^* (full lines) wavefunctions. We represent the modulus squared of the wavefunction averaged over planes perpendicular to the molecular “axis” represented as an inset (average charge in electron/bohr). This partial density averages to one for each state when integrated along the axis.

do not differ significantly, despite the very large difference in energy spectra. For the sake of illustration, we plot in Fig. 5 the LDA, COHSEX and Hartree-Fock σ_1 and π_2^* wavefunctions averaging the charge within planes perpendicular to the molecular “axis”. For the occupied σ_1 state, the LDA, COHSEX and Hartree-Fock wavefunctions (dotted lines) are nearly indistinguishable. However, for the π_2^* state (full lines), differences start to appear in particular at the Hartree-Fock level. Clearly, the COHSEX wavefunction is closer to the Kohn-Sham-LDA one, even though the COHSEX (and *GW*) quasiparticle spectrum is closer to the Hartree-Fock one.

The results of our *GW*/*BSE* study starting from self-consistent COHSEX eigenstates is presented in the column “@COHSEX” of Table I. As compared to *GW*/*BSE* calculations where the Kohn-Sham eigenstates are kept frozen (“@LDA” column), the *W1* and *W2* excitation energies hardly change by a maximum of 0.03 eV for the *W1* transition. The largest variation is again related to the *CTa* transition, with an increase of 0.22 eV, worsening the agreement with the CASPT2 value, but bringing our *GW*/*BSE* calculations in excellent agreement with the CAM-B3LYP ($\alpha + \beta = 0.8$) results. Such an evolution can be traced back to a ~ 0.2 eV blue-shift of the π_2^* energy level within *GW*@COHSEX as compared to *GW*@LDA. The oscillator strength associated with this transition is also seen to adopt a smaller value, worsening the agreement with the CASPT2 value, but improving

the agreement with the CAM-B3LYP result.

It is interesting to observe that what we may consider to be our most accurate values, namely our *GW*-Bethe-Salpeter calculations based on the COHSEX eigenstates, come in excellent agreement with the CAM-B3LYP value with enhanced long-range exchange, namely setting $(\alpha + \beta)$ to 0.8 instead of the original 0.65 value. We recall that in the case of CT excitations, the correct long-range "Mulliken" limit predicts a $(-1/D)$ scaling of the electron-hole binding energy, where D is some measure of the donor to acceptor distance. Such a behavior can only be reproduced with a $(\alpha + \beta = 1)$ parametrisation of the CAM-B3LYP functional. As such, the $(\alpha + \beta=0.8)$ functional provides in principle a better description of the long-range CT electron-hole interaction. Very consistently, the LC-BLYP functional, with a proper $(-1/D)$ asymptotic scaling, locates the *CTa* transition²² at 8.38 eV, in much better agreement with our *GW*/BSE values than the CASPT2 prediction. However, the analysis of the contributing wavefunctions in Fig. 5 shows that the *CTa* transition in the dipeptide is far from the ideal case of the long-range well-separated electron-hole CT limit. Overall, our *GW*/BSE@COHSEX results show a mean absolute error of 0.1 eV and 0.08 eV as compared to CAM-B3LYP $(\alpha + \beta = 0.8)$ and LC-BLYP, respectively.

Regarding previous studies on CT excitations within the present *GW*/BSE formalism, with typical errors of the order of 0.1 eV as compared to experiment, TDDFT with optimized range-separated functionals or CASPT2 calculations,^{42,43,45} the present 0.3 eV to 0.5 eV discrepancies for the *CTa* transition are somehow unusual, even though dramatically smaller than the typical errors induced by TDDFT calculation with semilocal kernels or even B3LYP. The 0.7 eV difference obtained between CAM-B3LYP calculations performed by the same authors with various parametrisations²² indicates that such variations cannot be explained by differences in running parameters (basis sizes and type, pseudopotential, etc.), but really hinges on the sensitivity of this transition onto the balance between short- and long-range exchange and correlation.

While we cannot comment on the accuracy and limitations of the available CASPT2 calculations, we certainly can emphasize in particular the lack of double-excitations in the present *GW*/BSE formalism and in TDDFT calculations, a possible explanation that would require more sophisticated treatments such as the inclusion of dynamical effects in the screened Coulomb potential matrix elements at the BSE level.¹⁰⁶ While this is certainly beyond the scope of the present paper, we can conclude that as it stands, the present parameter-free

GW/BSE approach offers an accuracy comparable to TDDFT calculations performed with the best available parametrized range-separated functionals.

IV. CONCLUSIONS

We studied within the many-body Green’s function *GW* and Bethe-Salpeter formalisms the excitation energies of a paradigmatic dipeptide that has served as a benchmark for describing intramolecular CT excitations in organic systems within various theoretical frameworks, including TDDFT with local, global hybrid and range-separated hybrid functionals, CASPT2 calculations and a previous Bethe-Salpeter study based on a model *GW* approach. In the present work, we performed fully *ab initio* *GW* calculations, evidencing important σ/π level reorderings as compared to the starting Kohn-Sham LDA energy spectrum. Based on *GW* calculations with partial self-consistency on the quasiparticle energies, our calculated Bethe-Salpeter excitation energies are found to agree with CASPT2 calculations with a discrepancy smaller than 0.07 eV for the local *W1*, *W2* and charge-transfer *CTb* excitations and a maximum discrepancy of 0.3 eV for the *CTa* transition. The effect of further updating self-consistently the quasiparticle wavefunctions within the static COHSEX approximation to *GW* leads to rather marginal variations for the *W1*, *W2* and *CTb* excitations, but shifts the discrepancy to 0.5 eV as compared to CASPT2 for the ubiquitous *CTa* transition. In fine, our BSE calculations based on the *GW*@COHSEX eigenvalues and eigenfunctions agree very well with both CAM-B3LYP calculations with enhanced long-range exchange ($\alpha + \beta = 0.8$) and the original LC-BLYP formulation, with a maximum mean absolute error of 0.1 eV. The present results allow to build confidence in the use of the present parameter-free *GW*/BSE formalism in describing local and charge-transfer excitations in organic systems of interest e.g. for photovoltaics, photosynthesis, or photocatalysis.

V. ACKNOWLEDGMENTS

C.F. acknowledges a joint CEA/CNRS BDI fellowship and P.B. a postdoctoral fellowship from the French national research agency under contract ANR-2012-BS04 PANELS. Computing time has been provided by the national GENGI-IDRIS supercomputing centers at Orsay under contract *n*^o i2012096655 and a PRACE european project under contract

n^o 2012071258. The authors are indebted to Prof. V. Robert and M. Verot for fruitful discussions concerning wavefunction based quantum chemistry approaches.

REFERENCES

- ¹N. S. Sariciftci, L. Smilowitz, A. J. Heeger, and F. Wudl, *Science* **258**, 1474 (1992).
- ²L. Schmidt-Mende, A. Fechtenkötter, K. Müllen, E. Moons, R. H. Friend, and J. D. MacKenzie, *Science* **293**, 1119 (2001).
- ³G. Li, R. Zhu, and Y. Yang, *Nat Photon* **6**, 153 (2012).
- ⁴A. A. Bakulin, A. Rao, V. G. Pavelyev, P. H. M. van Loosdrecht, M. S. Pshenichnikov, D. Niedzialek, J. Cornil, D. Beljonne, and R. H. Friend, *Science* **335**, 1340 (2012).
- ⁵D. Caruso and A. Troisi, *Proc. Natl. Acad. Sci.* **109**, 13498 (2012).
- ⁶S. R. Yost and T. Van Voorhis, *J. Phys. Chem. C* **117**, 5617 (2013).
- ⁷*Handbook of Computational Chemistry*, edited by J. Leszczynski (Springer Verlag Berlin Heidelberg, 2012).
- ⁸Q. Wu and T. Van Voorhis, *J. Chem. Theory Comput.* **2**, 765 (2006).
- ⁹P. Ghosh and R. Gebauer, *J. Chem. Phys.* **132**, 104102 (2010).
- ¹⁰E. Runge and E. K. U. Gross, *Phys. Rev. Lett.* **52**, 997 (1984).
- ¹¹M. A. L. Marques, C. Ullrich, F. Nogueira, A. Rubio, K. Burke, and E. K. U. Gross, *Time-Dependent Density Functional Theory* (Springer Verlag Berlin Heidelberg, 2006).
- ¹²M. E. Casida, *J. Mol. Struct.: THEOCHEM* **914**, 3 (2009).
- ¹³A. Dreuw, J. L. Weisman, and M. Head-Gordon, *J. Chem. Phys.* **119**, 2943 (2003).
- ¹⁴A. Dreuw and M. Head-Gordon, *J. Am. Chem. Soc.* **126**, 4007 (2004).
- ¹⁵D. J. Tozer, *J. Chem. Phys.* **119**, 12697 (2003).
- ¹⁶A. Savin, in *Recent Developments and Applications of Modern Density Functional Theory*, edited by J. M. Seminario (Elsevier, 1996).
- ¹⁷T. Leininger, H. Stoll, H.-J. Werner, and A. Savin, *Chem. Phys. Lett.* **275**, 151 (1997).
- ¹⁸J. Toulouse, F. Colonna, and A. Savin, *Phys. Rev. A* **70**, 062505 (2004).
- ¹⁹O. A. Vydrov, J. Heyd, A. V. Kruckau, and G. E. Scuseria, *The Journal of Chemical Physics* **125**, 074106 (2006).
- ²⁰H. Iikura, T. Tsuneda, T. Yanai, and K. Hirao, *J. Chem. Phys.* **115**, 3540 (2001).

- ²¹Y. Tawada, T. Tsuneda, S. Yanagisawa, T. Yanai, and K. Hirao, *J. Chem. Phys.* **120**, 8425 (2004).
- ²²T. Yanai, D. P. Tew, and N. C. Handy, *Chem. Phys. Lett.* **393**, 51 (2004).
- ²³R. Baer and D. Neuhauser, *Phys. Rev. Lett.* **94**, 043002 (Feb 2005).
- ²⁴L. Kronik, T. Stein, S. Refaely-Abramson, and R. Baer, *J. Chem. Theory Comput.* **8**, 1515 (2012).
- ²⁵T. Stein, L. Kronik, and R. Baer, *J. Am. Chem. Soc.* **131**, 2818 (2009).
- ²⁶B. M. Wong and J. G. Cordaro, *J. Chem. Phys.* **129**, 214703 (2008).
- ²⁷A. W. Lange, M. A. Rohrdanz, and J. M. Herbert, *J. Phys. Chem. B* **112**, 6304 (2008).
- ²⁸L. Hedin, *Phys. Rev.* **139**, A796 (1965).
- ²⁹G. Strinati, H. Mattausch, and W. Hanke, *Phys. Rev. Lett.* **45**, 290 (1980).
- ³⁰G. Strinati, H. Mattausch, and W. Hanke, *Phys. Rev. B* **25**, 2867 (1982).
- ³¹M. S. Hybertsen and S. G. Louie, *Phys. Rev. B* **34**, 5390 (1986).
- ³²R. W. Godby, M. Schlüter, and L. J. Sham, *Phys. Rev. B* **37**, 10159 (Jun 1988).
- ³³F. Aryasetiawan and O. Gunnarsson, *Rep. Prog. Phys.* **61**, 237 (1998).
- ³⁴W. G. Aulbur, L. Jönsson, and J. W. Wilkins, in *Solid State Physics*, edited by H. Ehrenreich and F. Spaepen (Academic Press, 1999).
- ³⁵L. J. Sham and T. M. Rice, *Phys. Rev.* **144**, 708 (Apr 1966).
- ³⁶W. Hanke and L. J. Sham, *Phys. Rev. Lett.* **43**, 387 (1979).
- ³⁷G. Strinati, *Phys. Rev. Lett.* **49**, 1519 (1982).
- ³⁸G. Strinati, *Rivista del nuovo cimento* **11**, 1 (1988).
- ³⁹M. Rohlfing and S. G. Louie, *Phys. Rev. Lett.* **80**, 3320 (1998).
- ⁴⁰L. X. Benedict, E. L. Shirley, and R. B. Bohn, *Phys. Rev. Lett.* **80**, 4514 (1998).
- ⁴¹S. Albrecht, L. Reining, R. Del Sole, and G. Onida, *Phys. Rev. Lett.* **80**, 4510 (1998).
- ⁴²X. Blase and C. Attaccalite, *Appl. Phys. Lett.* **99**, 171909 (oct 2011).
- ⁴³B. Baumeier, D. Andrienko, Y. Ma, and M. Rohlfing, *J. Chem. Theory Comput.* **8**, 997 (2012).
- ⁴⁴*Recent Progress in Coupled Cluster Methods*, edited by P. Cársky, J. Paldus, and J. Pittner, *Challenges and Advances in Computational Chemistry and Physics*, Vol. 11 (Springer Verlag Berlin Heidelberg, 2010).
- ⁴⁵C. Faber, I. Duchemin, T. Deutsch, and X. Blase, *Phys. Rev. B* **86**, 155315 (Oct 2012).
- ⁴⁶L. Serrano-Andres and M. P. Fuelscher, *J. Am. Chem. Soc.* **120**, 10912 (1998).

- ⁴⁷M. J. G. Peach, P. Benfield, T. Helgaker, and D. J. Tozer, *J. Chem. Phys.* **128**, 044118 (2008).
- ⁴⁸D. Rocca, D. Lu, and G. Galli, *J. Chem. Phys.* **133**, 164109 (2010).
- ⁴⁹B. Farid, R. Daling, D. Lenstra, and W. van Haeringen, *Phys. Rev. B* **38**, 7530 (1988).
- ⁵⁰M. L. Tiago and J. R. Chelikowsky, *Solid State Communications* **136**, 333 (2005).
- ⁵¹N. Dori, M. Menon, L. Kilian, M. Sokolowski, L. Kronik, and E. Umbach, *Phys. Rev. B* **73**, 195208 (May 2006).
- ⁵²M. Palumbo, C. Hogan, F. Sottile, P. Bagala, and A. Rubio, *J. Chem. Phys.* **131**, 084102 (2009).
- ⁵³N. Marom, X. Ren, J. E. Moussa, J. R. Chelikowsky, and L. Kronik, *Phys. Rev. B* **84**, 195143 (2011).
- ⁵⁴D. Foerster, P. Koval, and D. Sanchez-Portal, *J. Chem. Phys.* **135**, 074105 (2011).
- ⁵⁵G. Samsonidze, M. Jain, J. Deslippe, M. L. Cohen, and S. G. Louie, *Phys. Rev. Lett.* **107**, 186404 (2011).
- ⁵⁶S. Sharifzadeh, I. Tamblyn, P. Doak, P. Darancet, and J. Neaton, *Euro. Phys. J. B* **85**, 1 (2012).
- ⁵⁷P. Umari and S. Fabris, *J. Chem. Phys.* **136**, 174310 (2012).
- ⁵⁸N. Marom, F. Caruso, X. Ren, O. T. Hofmann, T. Körzdörfer, J. R. Chelikowsky, A. Rubio, M. Scheffler, and P. Rinke, *Phys. Rev. B* **86**, 245127 (2012).
- ⁵⁹T. Körzdörfer and N. Marom, *Phys. Rev. B* **86**, 041110 (2012).
- ⁶⁰T. A. Pham, H.-V. Nguyen, D. Rocca, and G. Galli, *Phys. Rev. B* **87**, 155148 (2013).
- ⁶¹X. Blase, C. Attaccalite, and V. Olevano, *Phys. Rev. B* **83**, 115103 (2011).
- ⁶²C. Faber, C. Attaccalite, V. Olevano, E. Runge, and X. Blase, *Phys. Rev. B* **83**, 115123 (2011).
- ⁶³A. Savin, in *Electron Correlation in the Solid State*, edited by N. March (World Scientific, Singapore, 1999).
- ⁶⁴O. Vahtras, J. Almlöf, and M. Feyereisen, *Chemical Physics Letters* **213**, 514 (1993).
- ⁶⁵X. Ren, P. Rinke, V. Blum, J. Wieferink, A. Tkatchenko, A. Sanfilippo, K. Reuter, and M. Scheffler, *New Journal of Physics* **14**, 053020 (2012).
- ⁶⁶F. Weigend and M. Hser, *Theoretical Chemistry Accounts* **97**, 331 (1997).
- ⁶⁷I. Cherkes, S. Klaiman, and N. Moiseyev, *Int. J. Quant. Chem.* **109**, 2996 (2009).

- ⁶⁸J. M. Soler, E. Artacho, J. D. Gale, A. García, J. Junquera, P. Ordeón, and D. Sanchez-Portal, *J. Phys.: Condens. Matter* **14**, 2745 (2002).
- ⁶⁹D. Ceperley and B. Alder, *Phys. Rev. Lett.* **45**, 566 (1980).
- ⁷⁰S. H. Vosko, L. Wilk, and M. Nusair, *Can. J. Phys.* **58**, 1200 (1980).
- ⁷¹J. P. Perdew and A. Zunger, *Phys. Rev. B* **23**, 5048 (1981).
- ⁷²N. Troullier and J. L. Martins, *Phys. Rev. B* **43**, 1993 (Jan 1991).
- ⁷³Similarly to strategies developed for post-Hartree-Fock correlated calculations, the first basis orbitals of the valence (s,p)-channels are taken to be the $2s$ and $2p$ eigenfunctions of isolated atoms in the corresponding pseudopotential approximation. The additional valence channels are taken to be two primitive Gaussians optimized to minimize the total energy at the DFT-LDA level. For carbon, the resulting most diffuse Gaussian present a decay coefficient $\alpha = 0.1 \text{ Bohr}^{-2}$, very close to the values optimized by Dunning at the cc-pVQZ level.⁷⁴ Following Ref. 68, the first d -channel orbital is taken to be the polarization orbital of the atomic p orbital, namely the d -component of the perturbation induced by a uniform electric field, complemented by a primitive Gaussian with decay constant $\alpha = 0.3 \text{ Bohr}^{-2}$ for carbon. Following Dunning, we finally add a single primitive Gaussian for the f -channel (with e.g. $\alpha = 0.76 \text{ Bohr}^{-2}$ for carbon).
- ⁷⁴T. H. Dunning, *J. Chem. Phys.* **90**, 1007 (1989).
- ⁷⁵F. Bruneval and M. A. L. Marques, *J. Chem. Theory Comput.* **9**, 324 (2013).
- ⁷⁶S. Sharifzadeh, A. Biller, L. Kronik, and J. B. Neaton, *Phys. Rev. B* **85**, 125307 (2012).
- ⁷⁷M. J. van Setten, F. Weigend, and F. Evers, *J. Chem. Theory Comput.* **9**, 232 (2013).
- ⁷⁸C. Faber, J. L. Janssen, M. Côté, E. Runge, and X. Blase, *Phys. Rev. B* **84**, 155104 (2011).
- ⁷⁹S. Ciuchi, R. C. Hatch, H. Höchst, C. Faber, X. Blase, and S. Fratini, *Phys. Rev. Lett.* **108**, 256401 (2012).
- ⁸⁰F. Bruneval, N. Vast, and L. Reining, *Phys. Rev. B* **74**, 045102 (2006).
- ⁸¹R. S. Mulliken, *Journal of the American Chemical Society* **74**, 811 (1952).
- ⁸²Y. Ma, M. Rohlfing, and C. Molteni, *Phys. Rev. B* **80**, 241405 (2009).
- ⁸³M. Grüning, A. Marini, and X. Gonze, *Nano Lett.* **9**, 2820 (2009).
- ⁸⁴I. Duchemin, T. Deutsch, and X. Blase, *Phys. Rev. Lett.* **109**, 167801 (2012).
- ⁸⁵We carefully tested the influence of the number of involved conduction bands on the resulting excitation energies and oscillator strengths. Between 120 and 160 conduction

bands, the excitation energies varied by less than 10 meV.

- ⁸⁶P. Giannozzi and al., *J. Phys. Condens. Matter* **21**, 395502 (2009).
- ⁸⁷A. Marini, C. Hogan, M. Gruning, and D. Varsano, *Comput. Phys. Comm.* **180**, 1392 (2009).
- ⁸⁸D. J. Tozer, R. D. Amos, N. C. Handy, B. O. Roos, and L. Serrano-Andres, *Mol. Phys.* **97**, 859 (1999).
- ⁸⁹Y. Akinaga and S. Ten-No, *Int. J. Quant. Chem.* **109**, 1905 (2009).
- ⁹⁰The structure we studied compares to structure 1a of Ref. 46, where results for different rotational structures of the dipeptide are presented.
- ⁹¹A. D. Becke, *J. Chem. Phys.* **98**, 1372 (1993).
- ⁹²M. J. Frisch, G. W. Trucks, H. B. Schlegel, G. E. Scuseria, M. A. Robb, J. R. Cheeseman, G. Scalmani, V. Barone, B. Mennucci, G. A. Petersson, H. Nakatsuji, M. Caricato, X. Li, H. P. Hratchian, A. F. Izmaylov, J. Bloino, G. Zheng, J. L. Sonnenberg, M. Hada, M. Ehara, K. Toyota, R. Fukuda, J. Hasegawa, M. Ishida, T. Nakajima, Y. Honda, O. Kitao, H. Nakai, T. Vreven, J. A. Montgomery, J. E. Peralta, F. Ogliaro, M. Bearpark, J. J. Heyd, E. Brothers, K. N. Kudin, V. N. Staroverov, R. Kobayashi, J. Normand, K. Raghavachari, A. Rendell, J. C. Burant, S. S. Iyengar, J. Tomasi, M. Cossi, N. Rega, J. M. Millam, M. Klene, J. E. Knox, J. B. Cross, V. Bakken, C. Adamo, J. Jaramillo, R. Gomperts, R. E. Stratmann, O. Yazyev, A. J. Austin, R. Cammi, C. Pomelli, J. W. Ochterski, R. L. Martin, K. Morokuma, V. G. Zakrzewski, G. A. Voth, P. Salvador, J. J. Dannenberg, S. Dapprich, A. D. Daniels, . Farkas, J. B. Foresman, J. V. Ortiz, J. Cioslowski, and D. J. Fox, "Gaussian 09 Revision A.1," Gaussian Inc. Wallingford CT 2009.
- ⁹³X. Qian, P. Umari, and N. Marzari, *Phys. Rev. B* **84**, 075103 (2011).
- ⁹⁴The HOMO-LUMO gap used to start the BSE calculations in Ref. 48 was opened to enforce the agreement between the TDLDA and BSE excitation energies for the local $W1$ transition. Due to the iterative methodology used in this previous work, the CTa transition with vanishing oscillator strength could not be obtained at the BSE level beyond the TDA.
- ⁹⁵The use of the Tamm-Dancoff approximation at the GW/BSE level leads to increased excitation energies and a deteriorated spectrum as compared to CASPT2. In agreement with the 0.15 eV blue shift reported by Rocca and coworkers,⁴⁸ the largest TDA induced shift

concerns the CTb excitation energy, which is blue-shifted by 0.17 eV in our calculations. The TDA further induces a small blue-shift of 0.03 eV for the $W1$ and $W2$ transitions, in perfect agreement with Ref. 48. The CTa charge-transfer state is marginally affected by a 0.01 eV blue-shift.

- ⁹⁶S. V. Faleev, M. van Schilfgaarde, and T. Kotani, Phys. Rev. Lett. **93**, 126406 (2004).
- ⁹⁷M. Shishkin and G. Kresse, Phys. Rev. B **75**, 235102 (2007).
- ⁹⁸C. Rostgaard, K. W. Jacobsen, and K. S. Thygesen, Phys. Rev. B **81**, 085103 (2010).
- ⁹⁹S.-H. Ke, Phys. Rev. B **84**, 205415 (2011).
- ¹⁰⁰F. Bruneval, J. Chem. Phys. **136**, 194107 (2012).
- ¹⁰¹M. Gatti, F. Bruneval, V. Olevano, and L. Reining, Phys. Rev. Lett. **99**, 266402 (2007).
- ¹⁰²J. Vidal, F. Trani, F. Bruneval, M. A. L. Marques, and S. Botti, Phys. Rev. Lett. **104**, 136401 (2010).
- ¹⁰³J. Vidal, S. Botti, P. Olsson, J.-F. Guillemoles, and L. Reining, Phys. Rev. Lett. **104**, 056401 (2010).
- ¹⁰⁴T. Rangel, D. Kecik, P. E. Trevisanutto, G.-M. Rignanese, H. Van Swygenhoven, and V. Olevano, Phys. Rev. B **86**, 125125 (2012).
- ¹⁰⁵The COHSEX, $GW@LDA$ and $GW@COHSEX$ LUMO energies are found to be 2.32 eV, 2.42 eV and 2.47 eV, respectively. This can be compared to the DFT-LDA starting Kohn-Sham value (-1.17 eV) and to the all-electron DFT-B3LYP 6-311G(d,p) Δ SCF value (2.13 eV) obtained with the Gaussian09 code.
- ¹⁰⁶D. Sangalli, P. Romaniello, G. Onida, and A. Marini, J. Chem. Phys. **134**, 034115 (2011).